ARTICLE

Growth Mechanism of Anisotropic Gold Nanocrystals *via* Microwave Synthesis: Formation of Dioleamide by Gold Nanocatalysis

Mona B. Mohamed,[†] Khaled M. AbouZeid, Victor Abdelsayed, Ahlam A. Aljarash, and M. Samy El-Shall*

Department of Chemistry, Virginia Commonwealth University, Richmond, Virginia 23284. [†]Permanent address: National Institute of Laser Enhanced Science, Cairo University, Cairo, Egypt.

ABSTRACT A facile and fast one-pot microwave irradiation method has been developed to prepare different shapes of gold nanoparticles capped with a mixture of oleylamine and oleic acid. The size, shape, and morphology of the nanocrystals could be tailored by varying the ratio of oleylamine to oleic acid, the microwave time, and the concentration of the gold ions. These effects are directly reflected in the surface plasmon resonance properties of the resulting nanocrystals in the visible and near-infrared regions. Pure amine leads to the formation of only spherical particles. Introducing oleic acid increases the growth rate and enhances the formation of anisotropic shapes. Experimental evidence and new insights on the reaction mechanism confirm the formation of dioleamide from the reaction of oleic acid and oleylamine catalyzed by the gold nanocrystals. In the absence of gold nanoparticles, the conventional synthesis of dioleamide requires 12 h of reaction time at 120 °C. New insights on the reaction mechanism indicate that excess oleic acid enhances the formation of hexagons and more anisotropic shapes of the gold nanocrystals.

KEYWORDS: gold nanocrystals · anisotropic shape · plasmon · growth mechanism · microwave irradiation · oleic acid · oleylamine · dioleamide

***Address correspondence to mselshal@vcu.edu.**

Received for review November 12, 2009 and accepted March 31, 2010.

Published online April 14, 2010.
10.1021/nn9016179

Gold nanocrystals are among the most studied nanoparticle systems due to their fascinating plasmonic and catalytic properties which can be tuned by controlling the particle size, shape, surface covering, and assembly of the individual nanocrystals.[1−4] Great recent interest has been focused on anisotropic gold nanocrystals because of their appealing optical properties.[4−9] The most interesting feature of the anisotropic shaped gold nanoparticles is that they have multiple absorption bands due to surface plasmon resonances (SPR) along their multiple axes.[6] For instance, gold nanorods exhibit two surface plasmon absorptions, the transverse and longitudinal resonances, due to oscillation of the surface electrons along the width and length of the rod, respectively.[10] However, the gold nanoprism has three absorption bands due to the in-plane dipole plasmon resonance, the in-plane quadrupole resonance, and the out-of-plane quadrupole resonance. The out-of-plane dipole resonance is sufficiently weak and broad that it is barely discernible as a shoulder on the in-plane resonance. The in-plane dipole plasmon resonance is very sensitive to the sharpness of the tips on the triangles.[11] In contrast, gold nanospheres, because of their symmetry, show only one surface plasmon band which is weakly dependent on the particle size. These unique optical properties of anisotropic gold nanocrystals enable the tuning of SPR to any wavelength specific to a particular application from the visible to the near-IR spectral regions. Using these nanomaterials in biomedical imaging,[12] cancer therapy and diagnosis,[13−16] catalysis,[17] sensors,[18] and photonic devices[19,20] is becoming a practical reality.

Microwave irradiation (MWI) is one of the most promising techniques for the preparation of nanomaterials with controlled size and shape since no high temperature or high pressure is needed.[21−26] The main advantage of MWI over other conventional heating methods is rapid and uniform heating of the reaction mixture. Due to the difference in the solvent and reactant dielectric constants, selective dielectric heating can provide significant enhancement in the transfer of energy directly to the reactants, which causes an instantaneous internal temperature rise. By using metal precursors that have large microwave absorption cross sections relative to the solvent, very high effective reaction temperatures can be achieved. This allows the rapid decomposition of the precursors, thus creating highly supersaturated solutions where nucleation and growth can take place to produce the desired nanocrystalline products. Since in MWI it is possible to quench

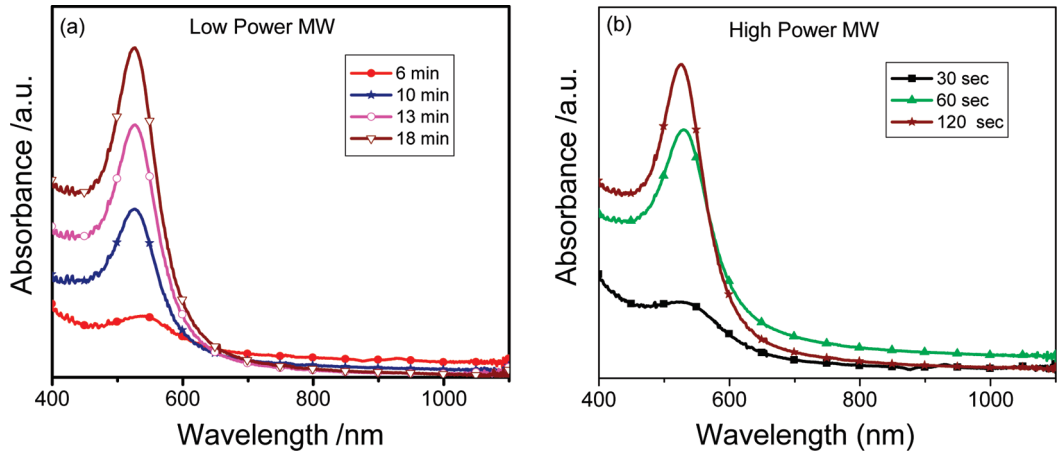

Figure 1. UV−vis spectra of Au nanoparticles prepared in pure oleylamine using (a) low microwave power (600 W) and (b) high microwave power (1000 W) irradiations at different reaction times.

the reaction very early on (~10 s), this provides the opportunity of controlling the nanostructures from small spherical nuclei to short rods to extended assemblies of nanowires, by varying the MWI reaction time and the relative concentrations of different organic surfactants with variable binding strengths to the initial precursors and to the nanocrystals. Although the MWI methods have been demonstrated for the synthesis of metallic nanoparticles such as gold, sliver, palladium, and platinum,[27−31] there are only a few reports for controlling the shape of the nanocrystals *via* MWI.[27−31] Our group has been able to produce semiconductor and metal oxide nanorods and wires using alkyl amines and mixtures of oleic acid (OAc) and oleylamine (OAm) as capping agents.[25−28] Very recently, Kundu *et al.*[32] reported a MWI method to synthesize multishaped gold nanoparticles in aqueous solution using 2,7-dihydroxy naphthalene as a reducing agent and cetyltrimethyl ammonium bromide (CTAB) as a capping material. While the role of CTAB and the formation mechanism of shape-controlled gold nanoparticles (*i.e.*, spheres, nanorods, and nanoprism) in aqueous solution are well-understood, controlling the shape of gold nanocrystals in an organic phase and understanding the growth mechanism are still not well-developed.

In this work, we developed a one-pot process using MWI to synthesize shape-controlled gold nanoparticles (*i.e.*, spherical, hexagons, truncated prisms, and prisms) in the presence of a mixture of OAm and OAc. The final particle shape and the growth rate depend on the ratio of the two surfactants as well as the concentration of gold ions and the MWI times. The present report is focused on studying the kinetic factors which affect the growth rate and on understanding the role of each capping material in the reaction mechanism. Furthermore, we provide direct evidence for the formation of dioleamide by the reaction of OAm and OAc catalyzed by the newly formed Au clusters under the MWI conditions.

RESULTS

When the Au^{3+} ions are reduced by pure OAm (no OAc added to the reaction mixture), only one plasmon band at 530 nm is observed due to the formation of spherical gold nanoparticles, as shown in Figure 1. This means that OAm could act as both a reducing agent and a capping material. The onset of the color change from yellow to pink corresponding to the formation of

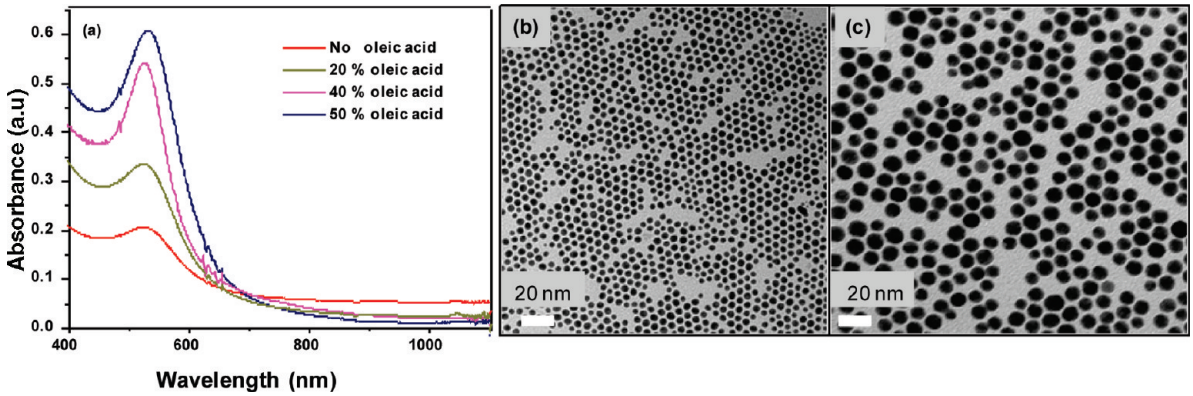

Figure 2. (a) UV−vis spectra for Au nanoparticles prepared using different ratios of oleic acid/oleylamine varied from 0 to 50% after 1 min MWI time. TEM images of gold nanoparticles prepared using pure amine (b) and in a 1:1 ratio of oleic acid/oleylamine (c). The scale bar is 20 nm.

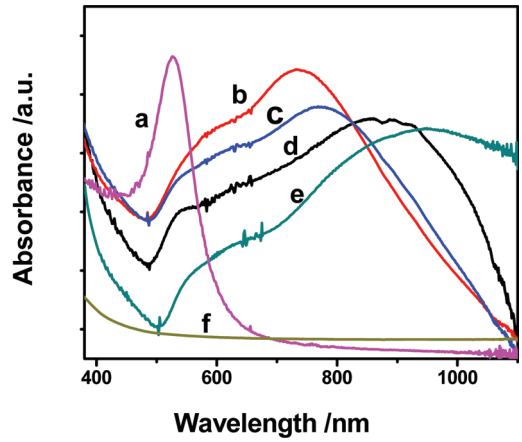

Figure 3. UV−vis spectra of the Au nanoparticles prepared with different molar ratios of oleic acid/oleylamine according to (a) 50, (b) 60, (c) 70, (d) 80, (e) 90, and (f) 100%.

the spherical Au nanoparticles varies from 30 s to a few minutes depending on the heating rate which is determined by the power of the MW oven used. As shown in Figure 1b, using a 1000 W MW oven, the reaction time can vary from 30 to 120 s.

A remarkable increase in the growth rate has been observed by introducing OAc into the reaction mixture. Figure 2 displays the absorption spectra of gold nanoparticles prepared in pure OAm and in different molar ratios of OAc to OAm (from 20% up to 50%) after 60 s reaction time using the 1000 W MW oven. The absorption spectra still show one absorption band at ~530 nm due to the SPR of the spherical gold nanoparticles. This is confirmed by imaging the particles prepared in pure OAm and in a 1:1 ratio of OAc to OAm using TEM. The TEM images displayed in Figure 2b and 2c show, in both cases, that the resulting nanoparticles are spherical but exhibit clearly different sizes. The average sizes of the particles prepared in pure OAm and in a 1:1 ratio OAc to OAm are ~8.0 ± 1.0 and 15.0 ± 2.0 nm, respectively. This indicates that the presence of OAc not only enhances the reaction rate of reducing the Au^{3+} ions to Au atoms and the formation of gold spherical particles but also increases the growth rate and the final particle size. No gold nanoparticles are formed in pure OAc even after MWI for more than 60 min. This confirms the assumption that the presence of the amine is responsible for the reduction of gold ions and the formation of the gold nanocrystals.

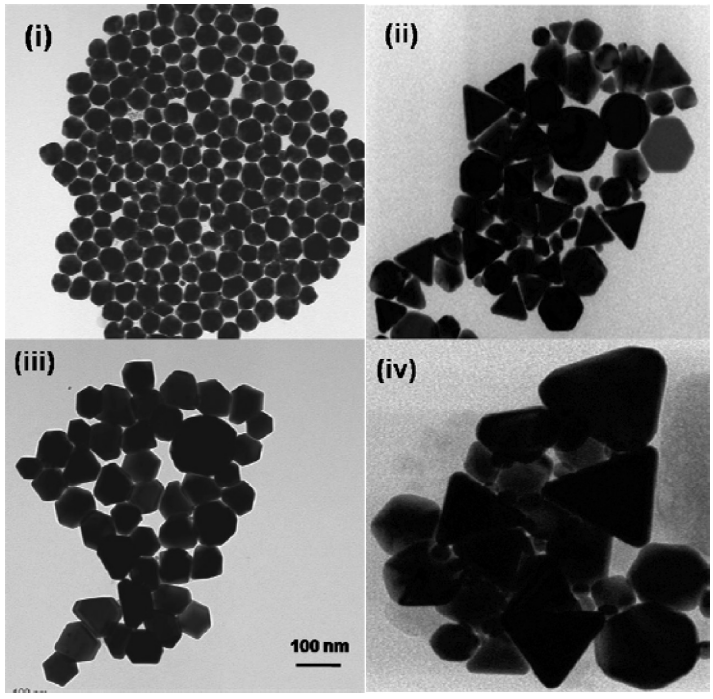

Figure 4. TEM images of the gold nanoparticles prepared in (i) 60, (ii) 70, (iii) 80, and (iv) 90% oleic acid.

Increasing the OAc ratio by more than 50% leads to remarkable color changes from red to purple to blue to gray green, accompanied by the appearance of new absorption features with gradual red shifts from the visible to the near-IR region. Figure 3 displays the absorption spectra of the gold nanocrystals prepared in (a) 50, (b) 60, (c) 70, (d) 80, (e) 90, and (f) 100% OAc. The new absorption bands are associated with the formation of anisotropic shaped gold nanoparticles and are red-shifted by increasing the ratio of OAc to OAm. A similar behavior has been observed for the longitudinal surface plasmon resonance of gold nanorods, which increases with larger aspect ratios.[6] In contrast, the transverse surface plasmon resonance of the nanorods does not depend on the aspect ratio and is at the same wavelength as the plasmon resonance of spheres.

TEM images show that increasing the ratio of OAc makes the particle's surface faceted and increases the particle size, as shown in Figure 4. Hexagons and truncated prisms are more predominate when the OAc ratio increases by more than 60%.

It was crucial to understand the reaction mechanism and the role of OAc because it enhances the reaction rate and affects the final shape of the nanocrystals. We studied the kinetic factors that could affect the growth rate, such as MWI time and the concentration of gold ions. The absorption spectra of the 60% molar ratio of OAc in the reaction mixture recorded at different MWI time intervals are shown in Figure 5 (top), and their TEM images obtained after different MWI times are shown in Figure 5 (bottom, a, b, and c). Consistent with the absorption spectra, the TEM images show the formation of Au spherical nanoparticles at early reaction times (Figure 5a), and that these small spheres start to form faceted surfaces and grow in size, as shown in Figure 5b,c.

If the molar ratio of OAc to OAm is less than 1:1, neither the concentration of gold ions nor the MWI time affect the final shape or the growth rate of the formed particles (see Supporting Information Figures S1 and S2). On the other hand, the concentration of the gold ions controls the particle size and shape in the presence of excess OAc (3:1 molar ratio of OAc/OAm). Figure 6

(top) displays the absorption spectra of the gold nanoparticles prepared in a 3:1 mixture of OAc and OAm using different concentrations of the gold ions. The TEM images displayed in Figure 6 (bottom, a and b) clearly indicate that increasing the concentration of the gold ions in the presence of excess OAc leads to the formation of larger nanocrystals with faceted surfaces and nearly hexagonal shapes.

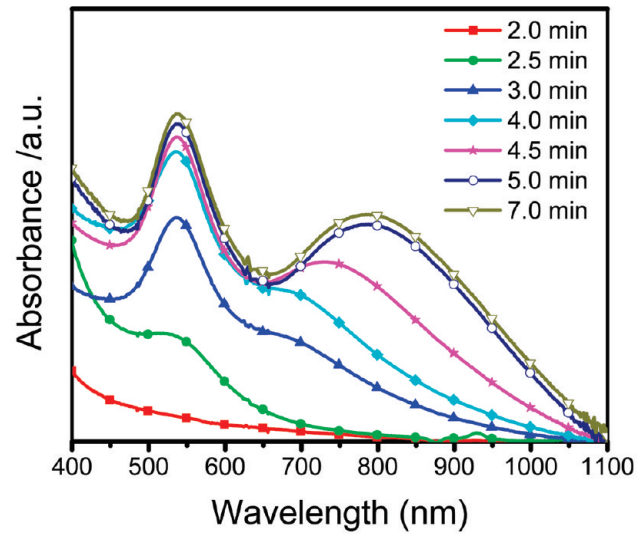

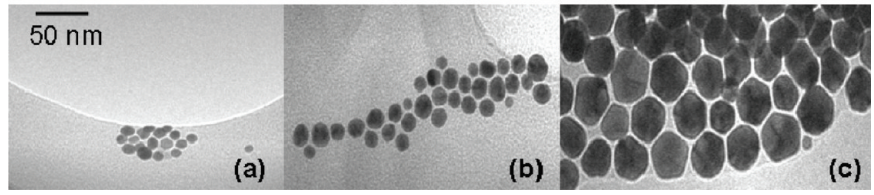

Figure 5. (Top) UV−vis absorption spectra of gold nanoparticles prepared in 60% oleic acid + 40% oleylamine at different microwave reaction times, and the corresponding TEM images (bottom) of the particles formed after (a) 2.5, (b) 4, and (c) 7 min MWI times.

DISCUSSION

To understand the mechanism of nanoparticle's formation and growth, it was important to study the nature of the interaction between OAc and OAm, and an OAc/OAm mixture in the presence of the gold ions. The FTIR spectra of pure OAc, pure OAm, and the reaction mixture consisting of OAc, OAm, and $HAuCl_4$ after MWI are shown in Figure 7. For comparison, the FTIR spectrum of oleamide purchased from Sigma-Aldrich is also included in Figure 7. Table S1 (Supporting Information) summarizes the observed IR bands of OAc, OAm, oleamide, and of the reaction mixture consisting of OAc, OAm, and $HAuCl_4$ after MWI.

The IR spectrum of the reaction mixture after MWI indicates that OAc reacts with OAm in the presence of the gold nanoparticles to form dioleamide, which is characterized by the presence of N−H bending at 1555 $cm^{-1}$and the C═O group shifted to 1695 cm^{-1}. Also, the disappearance of the NH_2 stretching at 3380 and 3313 cm^{-1} provides evidence for the formation of the amide. The C═O group of the OAc shows up as two bands in the dioleamide at 1695 and 1641 cm^{-1} because the amide group is usually present as a keto-amine tautomer.[33]

To further support the formation of dioleamide from the reaction of OAc and OAm in the presence of the gold ions, we prepared dioleamide separately by refluxing a 1:1 molar mixture of OAc, and OAm in anhydrous THF for 12 h at 120 °C.[34] The formed amide was separated from the reaction mixture and characterized by CHN elemental analysis, IR, and NMR. The experimental values of the CHN analysis (C% 81.72, H% 13.05, N% 2.58) are found to be in good agreement with the calculated values of the dioleamide (C% 81.35, H% 12.7, N% 2.63). Furthermore, we measured the ^1H NMR spectra of the prepared dioleamide, OAc, OAm, and the reaction mixture of OAc and OAm in the presence of gold ions (Supporting Information, Figure S3). The NMR spectrum of the prepared dioleamide shows a peak at δ 5.93 ppm due to the amide proton of the dialkylamide,[35,36] which is shifted to δ 5.60 ppm in the reaction mixture due to the interaction with the gold nanoparticles (Supporting Information, Figure S3). The ^1H NMR spectra of the dioleamide and the reaction mix-

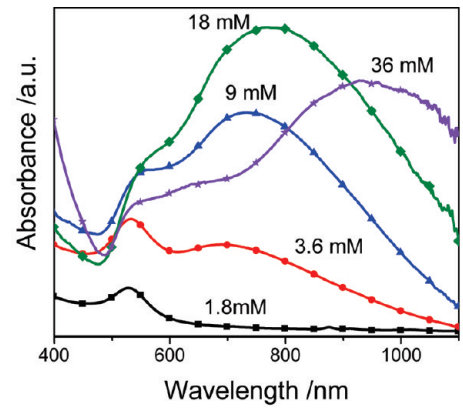

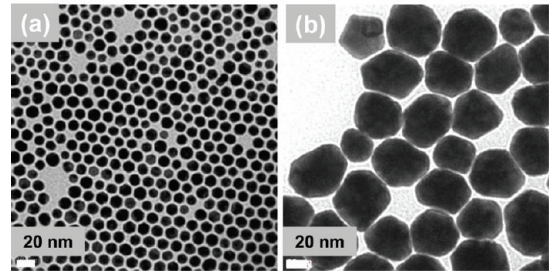

Figure 6. UV−vis absorption spectra of the gold nanoparticles formed in the presence of a 3:1 ratio of oleic acid/oleylamine using different concentrations of the gold ions as indicated, and TEM images of the gold nanoparticles formed using (a) 9 and (b) 36 mM of $HAuCl_4$.

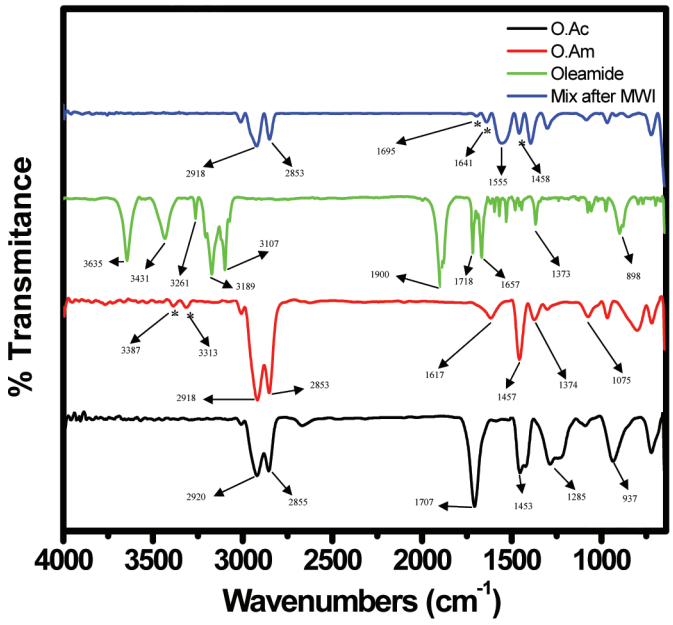

Figure 7. FTIR spectra of oleic acid (OAc), oleylamine (OAm), oleamide, and the reaction mixture consisting of OAc, OAm, and $HAuCl_4$ after MWI.

ture of the OAc, OAm, and the gold ions after MWI are very similar (Supporting Information, Figure S3). It is also important to note that the 1:1 molar mixture of OAc and OAm after MWI in the absence of the Au ions does not show the amide proton peak (Supporting Information, Figure S3). This indicates that the amide's formation is catalyzed by the small gold nanoparticles formed following the reduction of the gold ions. Thus, our suggested mechanism for the formation of the gold nanoparticles in a mixture of OAc and OAm is that OAm is the reducing agent for the Au ions; the nucleated Au nanoparticles catalyze the reaction between OAc and OAm to form dioleamide, which acts as a capping agent for the gold nanoparticle at the same time. The catalytic formation of the dioleamide is expected to be faster than adsorption of the dioleamide on the Au nanoparticles. Accordingly, the catalytic reaction is occurring on the small bare Au clusters formed by rapid nucleation following the supersaturation of the Au atoms in the solution induced by the MWI-assisted chemical reduction of the Au ions.

To prove our suggested mechanism, we used the dioleamide as both a reducing and a capping agent for the formation of gold nanoparticles under MWI. The absorption spectrum shows only one band at 523 nm due to the surface plasmon of the spherical nanoparticles, and the TEM image confirms this assignment as shown in Figure 8a. This is strong evidence that dioleamide can act as both a reducing and a capping agent, as well. To emphasize the role of the oleic acid as a key parameter in the growth of the anisotropic shapes of the gold nanoparticles, mixtures of dioleamide and oleic acid were used to prepare gold nanoparticles using the exact same conditions as before (*i.e.*, concentration of the gold ions, microwave power, and time). More control over the particle shape is obtained, as shown in Figure 8. The absorption spectra show a plasmonic band tunable from the visible to near-IR region, and the TEM images show that hexagonal-shaped particles appear to be predominant when using a 1:1 molar ratio of oleic acid and dioleamide (Figure 8b), while

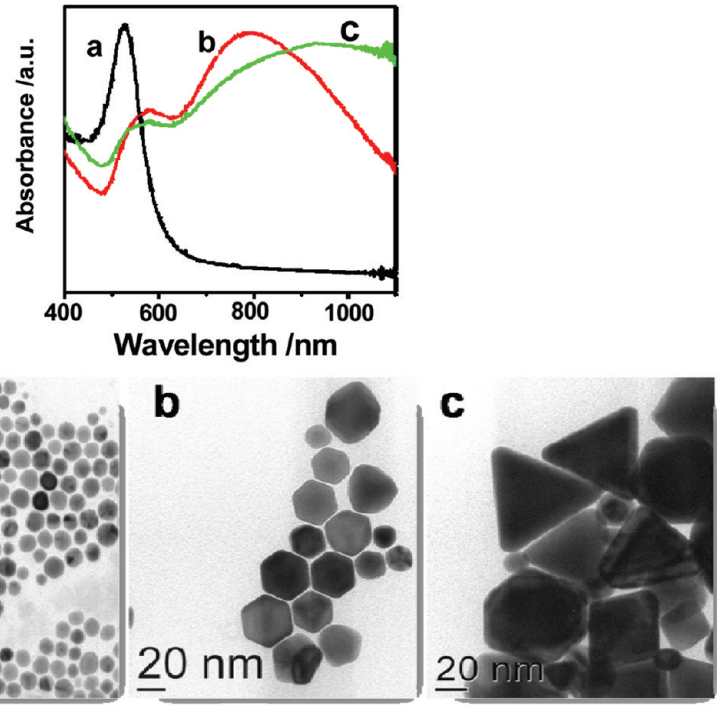

Figure 8. Absorption spectra and TEM images of the Au nanoparticles formed using (a) dioleamide only, (b) a 1:1 molar ratio of dioleamide and oleic acid, and (c) a 1:2 molar ratio of dioleamide and oleic acid.

prisms are more predominant when using a 2:1 molar ratio of oleic acid to dioleamide, as shown in Figure 8c.

According to the present results, we suggest the following mechanism for the formation of the nanoparticles using a mixture of OAm and OAc as a capping and reducing agent under microwave irradiation. OAc reacts with the OAm (1:1 molar ratio in the presence of the gold ions under MWI) forming dioleamide. Increasing the amount of OAc by more than 50% leads to an excess of free OAc in the reaction mixture. It is well-known that the spherical Au nanoparticles are characterized by two facets, (111) and (001).[37] The ratio between the growth of these two facets controls the final shape of the nanocrystals. These facets have different surface energies ($\sigma 111 < \sigma 100 < \sigma 110$).[38] The surface energy differences are responsible for the different bonding energies and chemical reactivity of the crystal faces. Since the (001) is more reactive and more polar than (111), it tends to adsorb the excess OAc on its surface more than the (111) facet. Oleic acid prevents more gold atoms to be ripened to this surface, thus hindering further growth of the (001) facet. This leads to increasing the growth rate of the [111] facet, which leads to the formation of hexagons and more anisotropic shapes.

CONCLUSIONS

In conclusion, this work develops a facile and fast one-pot microwave irradiation process for preparing shape-controlled anisotropic gold nanocrystals where the surface plasmon resonances can be tuned over the visible and near-IR spectral regions. The growth kinetics of the anisotropic gold nanocrystals can be controlled mainly by controlling the ratio of the oleic acid to oleylamine in the reaction mixture. Under the conditions where excess oleic acid is present, other parameters such as the concentration of the gold ions and the microwave irradiation time can be used to control the size, shape, and morphology of the resulting nanocrystals, which result in tuning the corresponding surface plasmon resonances. New insights on the reaction mechanism suggest that dioleamide is an effective reducing and capping agent and that excess oleic acid enhances the formation of hexagons and more anisotropic shapes of the gold nanocrystals.

METHODS

Typically, an appropriate amount of $HAuCl_4$ in HCl solution is mixed with a 1:1 molar ratio of OAm and OAc. The reaction mixture is stirred very well until it becomes homogeneous. After MWI of the clear solution for 30 s, the yellow color disappears. Continued microwaving for another 30 s leads to the formation of gold spherical particles which have a strong pink color. To understand the role of OAc and OAm, we prepared a series of solutions with different molar ratios of the OAm to OAc ranging from 0 to 100% OAc (pure amine, 80% amine, 60% amine, *etc.*, up to pure OAc). A fixed concentration of Au^{3+} ions was added to each solution followed by MWI until the yellow color disappeared and new colors due to the formation of different gold nanocrystals appeared. The optical absorption spectra for the resulting nanocrystals dispersed in toluene were measured using a HP-8453 spectrophotometer. Transmission electron microscopy (TEM) was carried out using a JEOL JEM-1230 electron microscope operated at 120 kV equipped with a Gatan UltraScan 4000SP 4K × 4K CCD camera. Samples for TEM were prepared by placing a droplet of a colloid suspension in toluene on a Formvar carbon-coated, 300-mesh copper grid (Ted Pella) and allowed to evaporate in air at room temperature. IR spectra were measured using a Nicole NEXUS 670 FTIR spectrophotometer. The spectra of OAc, OAm, oleamide, and the resulting reaction mixture with the obtained gold nanoparticles were measured by mixing one drop of the sample with KBr powder, which was then compressed to form a thin disk. The reaction between the oleylamine and oleic acid in the presence $HAuCl_4$ under MWI forming dioleamide was confirmed by ^1H NMR spectra and elemental analysis. The ^1H NMR spectra were measured using VARIAN NMR 300 MHz by dissolving the sample in $CDCl_3$. The CHN elemental analysis was performed to ensure the formation of the dioleamide by using a PerkinElmer 2400 Series II CHNS/O elemental analyzer.

Acknowledgment. We thank the NSF (CHE-0911146) for the support of this work.

Supporting Information Available: Effects of the concentration of the gold ions (Figure S1) and microwave time (Figure S2) on the growth of gold nanoparticles in a mixture of a 1:1 molar ratio of OAc/OAm. ^1H NMR spectra of (a) OAc, (b) OAm, (c) a 1:1 molar mixture of OAc and OAm after MWI with no gold ions present, (d) dioleamide prepared by the reaction of OAc and OAm at 120 °C for 12 h, and (e) a 1:1 molar mixture of OAc, OAm, and $HAuCl_4$ after MWI and the formation of gold nanoparticles (Figure S3). Table S1 summarizes the characteristic IR bands of oleic acid, oleylamine, and oleamide and the observed bands following the MWI of the reaction mixture. This material is available free of charge *via* the Internet at http://pubs.acs.org.

REFERENCES AND NOTES

1. Grzelczak, M.; Perez-Juste, J.; Mulvaney, P.; Liz-Marzan, L. M. Shape Control in Gold Nanoparticle Synthesis. *Chem. Soc. Rev.* **2008**, *37*, 1783–1791.
2. Eustis, S.; El-Sayed, M. A. Why Gold Nanoparticles are More Precious than Pretty Gold: Noble Metal Surface Plasmon Resonance and Its Enhancement of the Radiative and Nonradiative Properties of Nanocrystals of Different Shapes. *Chem. Soc. Rev.* **2006**, *35*, 209–217.
3. Burda, C.; Chen, X.; Narayanan, R.; El-Sayed, M. A. Chemistry and Properties of Nanocrystals of Different Shapes. *Chem. Rev.* **2005**, *105*, 1025–1102.
4. Treguer-Delapierre, M.; Majimel, J.; Mornet, S.; Duguet, E.; Ravaine, S. Synthesis of Non-Spherical Gold Nanoparticles. *Gold Bull.* **2008**, *41*, 195–207.
5. Millstone, J. E.; Wei, W.; Jones, M. R.; Yoo, H.; Mirkin, C. A. Iodide Ions Control Seed-Mediated Growth of Anisotropic Gold Nanoparticles. *Nano Lett.* **2008**, *8*, 2526–2529.
6. Harris, N.; Ford, M. J.; Mulvaney, P.; Cortie, M. B. Tunable Infrared Absorption by Metal Nanoparticles: The Case for Gold Rods and Shells. *Gold Bull.* **2008**, *41*, 5–14.
7. Kumar, P. S.; Pastoriza-Santos, I.; Rodriguez-Gonzalez, B.; Garcia de Abajo, F. J.; Liz-Marzan, L. M. High-Yield Synthesis and Optical Response of Gold Nanostars. *Nanotechnology* **2008**, *19*, 051606–051611.
8. Smith, D. K.; Korgel, B. A. The Importance of the CTAB Surfactant on the Colloidal Seed-Mediated Synthesis of Gold Nanorods. *Langmuir* **2008**, *24*, 644–649.
9. Sau, T. K.; Murphy, C. J. Room Temperature, High-Yield Synthesis of Multiple Shapes of Gold Nanoparticles in Aqueous Solution. *J. Am. Chem. Soc.* **2004**, *126*, 8648–8649.

10. Link, S.; Mohamed, M. B.; El-Sayed, M. A. Simulation of the Optical Absorption Spectra of Gold Nanorods as a Function of Their Aspect Ratio and the Effect of the Medium Dielectric Constant. *J. Phys. Chem. B* **1999**, *103*, 3073–3077.
11. Jin, R.; Cao, Y.; Mirkin, C. A.; Kelly, K. L.; Schatz, G. C.; Zheng, J. G. Photoinduced Conversion of Silver Nanospheres to Nanoprisms. *Science* **2001**, *294*, 1901–1903.
12. Hu, M.; Chen, J.; Li, Z.; Au, L.; Hartland, G. V.; Li, X; Marquez, M.; Xia, Y. Gold Nanostructures: Engineering Their Plasmonic Properties for Biomedical Applications. *Chem. Soc. Rev.* **2006**, *35*, 1084–1094.
13. El-Sayed, I.; Huang, X.; Macheret, F.; Humstoe, J. O.; Kramer, R.; El-Syaed, M. Effect of Plasmonic Gold Nanoparticles on Benign and Malignant Cellular Autofluorescence: A Novel Probe for Fluorescence Based Detection of Cancer. *Technol. Cancer Res. Treat.* **2007**, *6*, 403–412.
14. Dickerson, E. B.; Dreaden, E. C.; Haung, X.; El-Sayed, I. H.; Chu, H.; Pushpanketh, S.; McDonald, J. F.; El-Sayed, M. A. Gold Nanorod Assisted Near-Infrared Plasmonic Photothermal Therapy (PPTT) of Squamous Cell Carcinoma in Mice. *Cancer Lett.* **2008**, *269*, 57–66.
15. Huang, X.; Jain, P. K.; El-Sayed, I. H.; El-Sayed, M. A. Plasmonic Photothermal Therapy (PPTT) Using Gold Nanoparticles. *Lasers Med. Sci.* **2008**, *23*, 217–228.
16. Hirsch, L. R.; Stafford, R. J.; Bankson, J. A.; Sershen, S. R.; Rivera, B.; Rrice, R. E.; Hazle, J. D.; Halas, N. J.; West, J. L. Nanoshell-Mediated Near-Infrared Thermal Therapy of Tumors under Magnetic Resonance Guidance. *Proc. Natl. Acad. Sci. U.S.A.* **2003**, *100*, 13549–13554.
17. Loo, C.; Lin, A.; Hirsch, L.; Lee, M.; Barton, J.; Halas, N., J.; West, J.; Drezek, R. Nanoshell-Enabled Photonics-Based Imaging and Therapy of Cancer. *Technol. Cancer Res. Treat.* **2004**, *3*, 33–40.
18. Bi, Y.; Lu, G. Morphological Controlled Synthesis and Catalytic Activities of Gold Nanocrystals. *Mater. Lett.* **2008**, *62*, 2696–2699.
19. Haes, A. J.; Hall, W. P.; Chang, L.; Klein, W. L.; Van Duyne, R. P. A Localized Surface Plasmon Resonance Biosensor: First Steps toward an Assay for Alzheimer's Disease. *Nano Lett.* **2004**, *4*, 1029–1034.
20. Ueno, K; Yokota, Y; Juodkazis, S; Mizeikis, V; Misawa, H. Nano-Structured Materials in Plasmonics and Photonics. *Curr. Nanosci.* **2008**, *4*, 232–235.
21. Zhu, J.; Palchik, O.; Chen, S.; Gedankan, A. Microwave Assisted Preparation of CdSe, PbSe, and $Cu_{2-x}Se$ Nanoparticles. *J. Phys. Chem. B* **2000**, *104*, 7344–7347.
22. Gallis, K.; Landry, C. Rapid Calcination of Nanostructured Silicate Composites by Microwave Irradiation. *Adv. Mater.* **2001**, *13*, 23–26.
23. Liang, J.; Deng, Z. X.; Jiang, X.; Li, F.; Li, Y. Photoluminescence of Tetragonal ZrO_2 Nanoparticles Synthesized by Microwave Irradiation. *Inorg. Chem.* **2002**, *41*, 3602–3604.
24. Gerbec, J. A; Magana, D.; Washington, A.; Strouse, G. F. Microwave-Enhanced Reaction Rates for Nanoparticle Synthesis. *J. Am. Chem. Soc.* **2005**, *127*, 15791–15800.
25. Panda, A. B.; Glaspell, G. P.; El-Shall, M. S. Microwave Synthesis of Highly Aligned Ultra Narrow Semiconductor Rods and Wires. *J. Am. Chem. Soc.* **2006**, *128*, 2790–2791.
26. Panda, A. B.; Glaspell, G. P.; El-Shall, M. S. Microwave Synthesis and Optical Properties of Uniform Nanorods and Nanoplates of Rare Earth Oxides. *J. Phys. Chem. C* **2007**, *111*, 1861–1864.
27. Abdelsayed, V.; Panda, A. B.; Glaspell, G. P.; El-Shall, M. S. In *Nanoparticles: Synthesis, Stabilization, Passivation, and Functionalization*, ACS Symposium Series 996; Nagarajan, R., Hatton, A. T., Eds.; American Chemical Society: Washington, DC, 2008; Chapter 17, pp 225−247.
28. Abdelsayed, V.; Aljarash, A.; El-Shall, M. S.; Al Othman, Z. A.; Alghamdi, A. H. Microwave Synthesis of Bimetallic Nanoalloys and CO Oxidation on Ceria-Supported Nanoalloys. *Chem. Mater.* **2009**, *21*, 2825–2834.
29. Harpeness, R.; Gedanken, A. Microwave Synthesis of Core−Shell Gold/Palladium Bimetallic Nanoparticles. *Langmuir* **2004**, *20*, 3431–3434.
30. Pastoriza-Santos, I.; Liz-Marzán, L. Formation of PVP-Protected Metal Nanoparticles in DMF. *Langmuir* **2002**, *18*, 2888–2894.
31. Chen, W.; Zhao, J.; Lee, J. Y.; Liu, Z. Microwave Heated Polyol Synthesis of Carbon Nanotubes Supported Pt Nanoparticles for Methanol Electrooxidation. *Mater. Chem. Phys.* **2005**, *91*, 124–129.
32. Kundu, S.; Peng, L.; Liang, H. A New Route to Obtain High-Yield Multiple-Shaped Gold Nanoparticles in Aqueous Solution Using Microwave Irradiation. *Inorg. Chem.* **2008**, *47*, 6344–6352.
33. http://www.cem.msu.edu/~reusch/VirtTxtJml/Spectrpy/InfraRed/infrared.htm.
34. Visek, K. E. In *Cationic Surfactants in Organic Chemistry*, Surfactant Science Series; Richmond, J. M., Ed.; CRC Press: Boca Raton, FL, 2001; Vol. 34, Chapter 1.
35. Vandevoorde, S.; Jonsson, K.-O; Foler, C. J.; Lambert, D. M. Modifications of the Ethanolamine Head in *N*-Palmitoylethanolamine: Synthesis and Evaluation of New Agents Interfering with the Metabolism of Anandamide. *J. Med. Chem.* **2003**, *46*, 1440–1448.
36. http://www.cem.msu.edu/~reusch/VirtualText/Spectrpy/nmr/nmr1.htm.
37. Wang, Z. L.; Mohamed, M. B.; Link, S.; El-Sayed, M. A. Crystallographic Facets and Shapes of Gold Nanorods of Different Aspect Ratios. *Surf. Sci.* **1999**, *440*, L809–L814.
38. Wang, Z. L. Transmission Electron Microscopy of Shape-Controlled Nanocrystals and Their Assemblies. *J. Phys. Chem. B* **2000**, *104*, 1153–1175.